APPLICATION OF ANGLE-DEPENDENCE IN THE ULTRASONIC ECHO SIGNAL TO ESTIMATION OF CAROTID PLAQUE CONTENTS

Jens E. Wilhjelm[1], Marie-Louise M. Grønholdt[2] and Henrik Sillesen[3]

Center for Arteriosclerosis Detection with Ultrasound (CADUS). E-mail: wilhjelm@it.dtu.dk. Homepage: http://www.it.dtu.dk/~wilhjelm/cadus.html.
[1]Department of Information Technology, Technical University of Denmark, Building 344, DK-2800 Lyngby, Denmark.
[2]Department of Vascular Surgery, Rigshospitalet, University of Copenhagen, Blegdamsvej 9, DK-2100 Copenhagen Ø, Denmark.
[3]Department of Vascular Surgery, Gentofte Hospital, University of Copenhagen, DK-2900 Hellerup, Denmark.

INTRODUCTION

Ultrasound imaging of the carotid arteries is today the prevailing method for clinical diagnosis of arteriosclerosis in the carotid arteries. The degree of stenosis can be estimated from the blood velocity image and the appearance of the plaque itself can be assessed from the anatomical B-mode image. Both pieces of information are used to assess the risk of plaque rupture, which - through the production of emboli - can lead to stroke. In particular, recent research has demonstrated that the B-mode image reveals features related to the risk of development of future neurological symptoms and brain infarcts.[1] These image features are related to plaque material and structure, but determination of this relationship is very difficult with the current imaging technique.

The arteriosclerotic plaque mainly consist of five material constituents: thrombus, haemorrhage, lipid materials, fibrous tissues and calcification. The first three constituents probably cannot be distinguished by ultrasound and are typically categorized as "soft materials". The remaining material groups (soft materials, fibrous tissues and calcification) are normally associated with increasing echogenicity with increasing dependence of insonification angle. A clear demonstration of this behavior was made by *Picano et al*:[2] For fatty wall, fibrofatty wall, fibrous wall and calcified wall the maximal backscattering coefficient as a function of angle and the degree of the angular dependence increased.

In contrast to the presumably slap-like shape of the opened aorta wall, the carotid plaques investigated in the present study have a more pronounced three dimensional structure. To fully account for this, three-dimensional ultrasound images were recorded from five different angles, features measuring the angle-dependence in these images were calculated and the results compared to quantitative histological analysis.

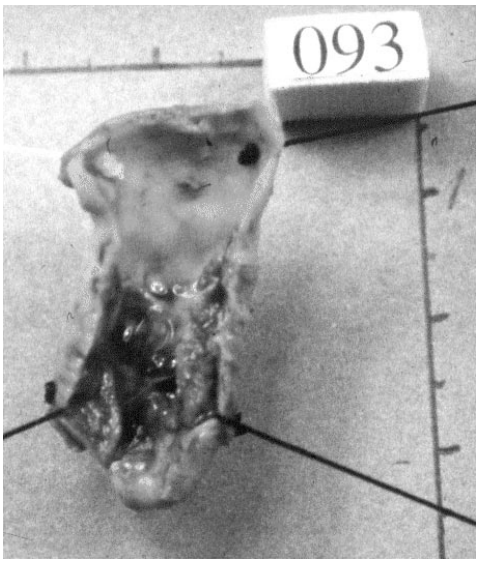

Figure 1 Carotid plaque after surgical removal, fixed with four sutures mounted to an acrylic frame (not shown). The two axes have tick marks every 0.5 cm.

MATERIALS AND METHODS

Plaque Materials

Plaques from thirteen patients with carotid artery disease were removed by prophylactic carotid endarterectomy.[3] All patients were referred to the Department of Vascular Surgery, Rigshospitalet, Copenhagen, with neurological symptoms from the same side as the stenotic carotid artery. Immediately after removal from the patients, the plaques were fixed in formalin. The subsequent *in vitro* scanning was carried out within 2 weeks. The longitudinally opened plaques were fixed to an acrylic frame in an "as open as possible" condition by means of four sutures, as illustrated in Figure 1. The frame with plaque was next inserted into a thin-walled latex bag with formalin. The plaques had to remain in formalin during scanning, as this could take up to 24 hours.

Histological Analysis

Following ultrasound scanning (to be described subsequently), sutures were removed from the plaques which were subsequently laced back into a shape that matched the *in vivo* form as close as possible. The features analyzed were the volumetric contents of soft materials, fibrous tissues and calcification. The total relative content were 26.9 ±10.1 %, 72.5 ±9.9 % and 0.7 ±0.5 % (mean ± standard deviation), respectively.

Ultrasound System

The experimental ultrasound system consisted of a pulser/receiver driving a 10 MHz, 0.25" diameter, single element spherically focused (at 40 mm) ultrasound transducer. As illustrated in Figure 2, the transducer was mounted to a manual rotational device, such that the ultrasound beam intersected the axis of rotation at a distance of D_{rot} = 58.5 mm. Thus measurements took place in the far field, where the energy of the received signal from a plane reflector - as a function of insonification angle - has a more simple behavior (e.g. Gaussian shaped) than at the near field. The rotational device holding the transducer could be translated in three orthogonal directions. For the purpose of noise reduction, fifty received signals obtained from the same spatial position were averaged in the digital oscilloscope. Also a bandpass filter was applied in the computer to further reduce noise outside the transducer passband.

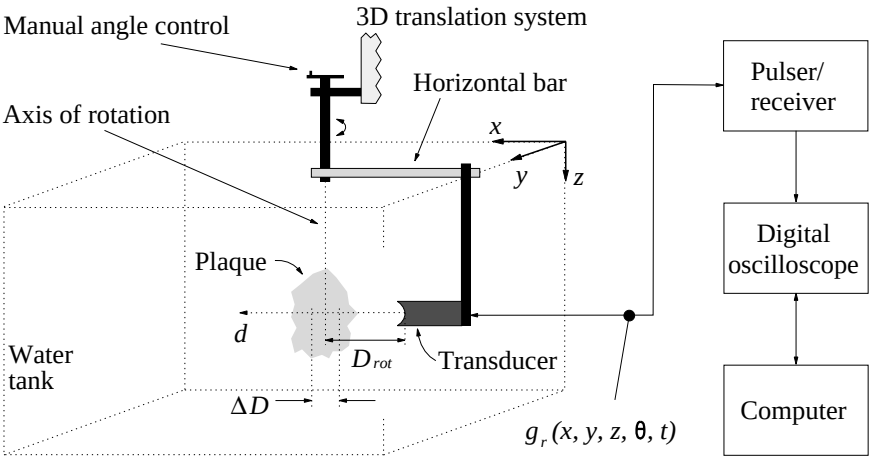

Figure 2 Single element spherically focused ultrasound transducer mounted to rotation axis via a horizontally mounted bar. The rotational system could be translated in space. The acoustic axis intersects the axis of rotation at an angle of 90˚.

The beamwidth of the ultrasound transducer was characterized using a 0.1 mm diameter glass sphere moulded into an agar block. At the range D_{rot}, the –3 dB lateral beamwidth was found to 1.4 mm.

To ensure that the ultrasound beam intersected the translation axis as indicated in Figure 2, a special line reflector could be mounted to the physical part of the rotational axis, which was a 13 mm in diameter rod. The line reflector was made from 0.1 mm in diameter stainless steel wire mounted with high precision so that it coincided with the axis of rotation within 0.1 mm. With the line reflector in place, the transducer fixation could be adjusted so that the acoustic axis intersected the axis of rotation.

Recording Procedure

The same part of the ultrasound beam was used for all range cells which required the rotational system with transducer moved in 3D to each specific range cell. The advantage of this time consuming approach was high precision in the spatial definition of the range cell and that all range cells were insonified exactly the same way. The received signal segment, $g_r(x, y, z, \theta, t)$, for a given range cell, (x, y, z) and angle, θ, was extracted by windowing out a small segment from the entire received signal. This segment was located from $T_{rot} - T_w/2$ to $T_{rot} + T_w/2$, where $T_{rot} = 2D_{rot}/c$ and $T_w = \Delta D/c$ is the window length ($\Delta D \sim 4$ mm).

Generation of 3D Energy Images

In order to obtain range cells with an omnidirectional sensitivity function, the axial resolution size had to be made equal to the lateral resolution size. This was done by multiplying the received signal segment, $g_r(x, y, z, \theta, t)$, from each range cell with a Gaussian window. The –3 dB length of this window, $T_{\text{-3dB}}$, roughly corresponded to the –3 dB width of the ultrasound beam at D_{rot} (*i.e.*, 1.4 mm). Thus the axial resolution was degraded by this procedure. The result of the multiplication was then integrated in order to calculate the energy of the received signal as a function of spatial location and angle

$$E(x,y,z,\theta) = \int_{-T_w/2}^{T_w/2} \left| \exp\left[-\frac{2\ln(2)}{T_{-3dB}^2}\left(t - \frac{T_{rot}}{2} \right)^2 \right] g_r(x,y,z,\theta,t) \right|^2 dt \qquad (1)$$

Thus, for a given θ, $E(x, y, z, \theta)$ constitutes a 3D energy image.

Evaluation of Spatial Calibration

The precision of the combined rotation and translation system was investigated with the point target. 3D energy images (15x15x15 range cells) of the point target were recorded from the three angles $\theta = -20^\circ$, 0°, and 20°. From these three 3D images, the 3D "point of gravity" (corresponding in 1D to the centroid of *e.g.* a spectrum) was calculated. The three estimated 3D locations should coincide. Comparing them revealed that the maximal spatial difference was below 0.25 mm or less than two wavelengths.

Feature Extraction

Before the 3D energy images of the plaques could be used, the range cells containing sutures had to be masked out manually. Consider a given range cell in a set of five 3D energy images. In Figure 3 it is illustrated how the five associated energy values can be used to calculate six simple features for that cell. In this paper, the "feature volume images" were reduced to single scalars by means of averaging. If N_q is the number of range cells representing plaque, $N_{\theta,q}$ is the number of insonification angles for plaque q, and $\Delta\theta$ is the insonification angle increment, then the three features based on change in energy over angle can be written as:

$$F_{S,\min}(q) = \frac{1}{N_q} \sum_{x,y,z} \min_{\theta} \left(\frac{|E(x,y,z,\theta) - E(x,y,z,\theta+\Delta\theta)|}{\Delta\theta} \right)$$

$$F_{S,mean}(q) = \frac{1}{N_q} \sum_{x,y,z} \frac{1}{N_{\theta,q}-1} \sum_{\theta} \left(\frac{|E(x,y,z,\theta) - E(x,y,z,\theta+\Delta\theta)|}{\Delta\theta} \right) \quad (2)$$

$$F_{S,\max}(q) = \frac{1}{N_q} \sum_{x,y,z} \max_{\theta} \left(\frac{|E(x,y,z,\theta) - E(x,y,z,\theta+\Delta\theta)|}{\Delta\theta} \right)$$

where $\theta = -20^\circ$, -10°, -0°, 10° (for $N_{\theta,q} = 5$). The remaining three features based on energy can be written as:

$$F_{E,\min}(q) = \frac{1}{N_q} \sum_{x,y,z} \min_{\theta}(E(x,y,z,\theta))$$

$$F_{E,mean}(q) = \frac{1}{N_q} \sum_{x,y,z} \frac{1}{N_{\theta,q}} \sum_{\theta} E(x,y,z,\theta) \quad (3)$$

$$F_{E,\max}(q) = \frac{1}{N_q} \sum_{x,y,z} \max_{\theta}(E(x,y,z,\theta))$$

where $\theta = -20^\circ$, -10°, -0°, 10° and 20° (for $N_{\theta,q} = 5$).

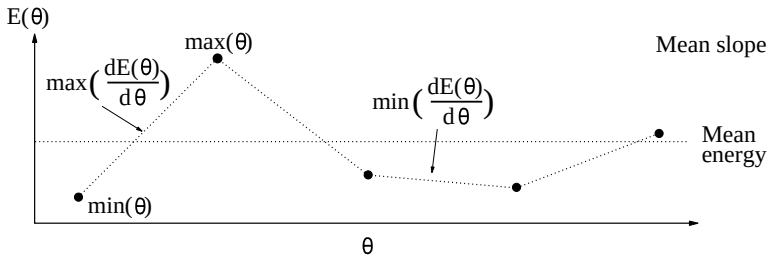

Figure 3 Five energy values from a given range cell, plotted as a function of angle. Six different features can be calculated based on these energy values.

Table 1 Overview of feature performance parameters.

Type	ε_{rms}	p	r
$F_{S,min}$	0.05	0.0002	0.86
$F_{S,mean}$	0.07	0.02	0.63
$F_{S,max}$	0.08	0.09	0.49
$F_{E,min}$	0.06	0.001	0.80
$F_{E,mean}$	0.06	0.004	0.74
$F_{E,max}$	0.07	0.02	0.64

RESULTS

3D energy images were recorded for thirteen plaques. The distance between the center of neighboring range cells was 1.4 mm and signals from approximately 1000 range cells were recorded for each plaque.

The correlation between the histologically determined relative content of fibrous materials, represented in vector $\underline{Y}$, and one of the six ultrasound features, contained in matrix $\underline{\underline{X}}$, were investigated using the linear model, $\underline{Y} = \underline{\underline{X}}\ \underline{\beta}$. The regression parameters, $\underline{\hat{\beta}}$, were found based on the least-squares solution. The *rms* error (residual) is: $\varepsilon_{rms} = E\{(\underline{Y} - \underline{\underline{X}}\ \underline{\hat{\beta}})^2\}^{1/2}$, where E{} extracts the mean value.

The *rms* error, the *p*-value and the correlation coefficient, *r*, for the six features are show in Table 1. The feature values were scaled to best match the relative content of fibrous materials, and a comparison between these for all plaques are show in Figure 4. To ease interpretation, the plaques were sorted in ascending order with respect to relative content of fibrous tissues.

DISCUSSION

The preliminary results in Table 1 and Figure 4 suggest that $F_{S,min}$, $F_{E,min}$ and $F_{E,mean}$ correlated well to the histologically determined relative content of fibrous tissues.

The plaques in the present study mainly consist of soft materials and fibrous tissues. Therefore, based on the results of Picano[2], it should be expected that the energy (averaged over space and angles) as well as the angular dependence increases with relative content of fibrous materials. This was the case for all features.

Despite the good preliminary results presented in this paper, a number of sources of error exist, which should be kept in mind when evaluating the performance of the method:

a) The plaque was only scanned over an angle interval of 40˚ in one plane. For the 3D-shaped plaques investigated in the present study, perpendicular incidence (to the degree it can be defined) does not happen for all range cells.

b) For the above reason, the rather simple feature extraction scheme might not be optional and other approaches should be investigated as well.

c) The histological classification used might not be completely in agreement with ultrasonic behavior. The tissue class "fibrous tissues" covers a large range of tissues, which might not all behave as "strong" reflectors.

d) Finally, there is a general uncertainty on the histological results. First, sections were cut with a coarse spatial sampling interval of 3 mm. Second, the histological constituents were often mixed, making drawing of exact borders difficult.

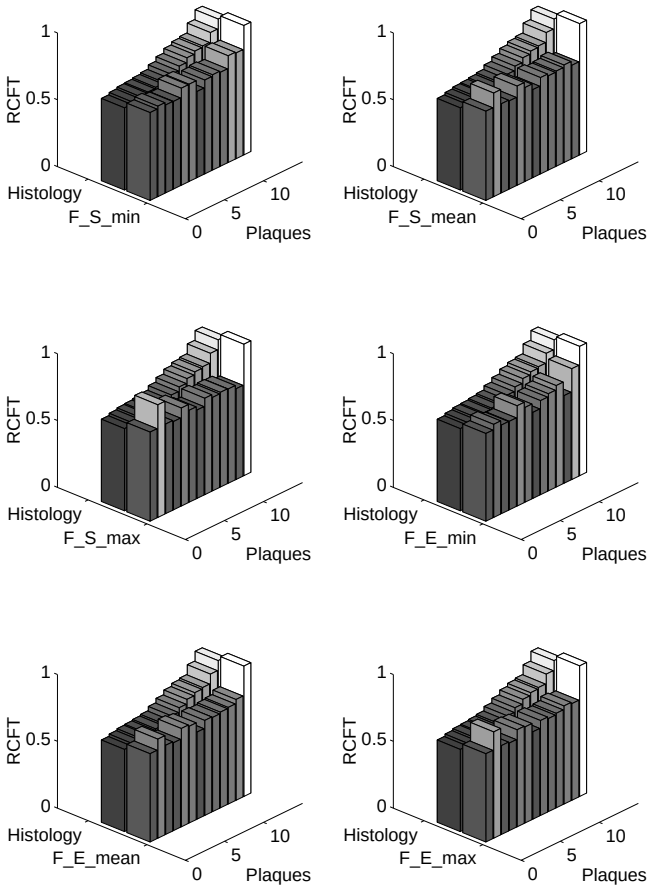

Figure 4 Relative content of fibrous tissues compared to scaled value of ultrasound feature. The plaques are sorted according to the former. RCFT = Relative Content of Fibrous Tissues.

CONCLUSIONS

Thirteen plaques, removed by carotid endarterectomy, have been scanned with ultrasound in 3D from five different insonification angles. The results of the scanning were 3D images representing received ultrasound energy as a function of angle. Six features were extracted from these 3D images and correlated with the histologically determined relative content of fibrous tissue. Good correlation were found for three of these different features.

ACKNOWLEDGEMENTS

CADUS is partly supported by the Danish Technical and Medical Research Councils. The authors gratefully acknowledge the help by M.S. Student Niels Nordmann in carrying out part of the measurements.

REFERENCES

[1] *Cave EM, Pugh ND, Wilson RJ, Sissons GRJ, Woodcock JP:* **Carotid artery duplex scanning: Does plaque echogenicity correlate with patient symptoms?** Eur. J. Vasc. Endovasc. Surg. Vol.10. pp.77-81. 1995.

[2] *Picano E, Landini L, Distante A, Salvadori M, Lattanzi F, Masini M and L'Abbate A:* **Angle dependence of ultrasonic backscatter in arterial tissues: a study in vitro.** Circulation, vol.72, no.3, pp.572-576. 1985.

[3] *Wilhjelm JE, Grønholdt M-LM, Rasmussen S, Martinsen K and Sillesen H*: **Estimation of Plaque Contents With Multi-Angle 3D Compound Imaging**. Proc. of the IEEE International Ultrasonics Symposium, San Antonio, November 3-6, 1996.